Nuclear Materials and Energy 18 (2019) 345–349

Contents lists available at ScienceDirect

Nuclear Materials and Energy

journal homepage: www.elsevier.com/locate/nme

Adhesion force of W dust on tokamak W plasma-facing surfaces: The importance of the impact velocity

A. Autricque[*,a], F. Gensdarmes[b], S. Peillon[b], M. Sow[b], C. Grisolia[a,c]

[a] CEA, IRFM, F-13108, Saint-Paul-Lez-Durance, France
[b] Institut de Radioprotection et de Sûreté Nucléaire (IRSN), Gif-sur-Yvette 91192, France
[c] National Research Nuclear University "MEPhI", Moscow 115409, Russian Federation

ABSTRACT

The adhesion of tungsten (W) dust particles on W tokamak plasma-facing surfaces is investigated. When spherical dust hits the tokamak walls, its shape is altered as a contact area is created by the adhesion work and irreversible plastic deformation. The van der Waals adhesion force between such a deformed grain and a flat surface is estimated, and the link between the force and the impact velocity is determined. We show that adhesion can be increased by several orders of magnitude when the impact velocity approaches the adhesion velocity. Finally, the effects of surface roughness are incorporated.

1. Introduction

Due to the toroidal shape of tokamaks, dust transported in fusion plasmas tend to be accelerated towards the vacuum vessel outer walls. The outcome (adhesion, rebound or destruction) of dust-wall collisions, as well as the estimation of adhesion forces, are critical to the quantification of dust sources and sinks in fusion devices. This makes dust-wall collisions a crucial issue to address in any dust modelling code [1–6]. A dust-wall impact is generally decomposed into its normal and tangential components since they involve different physics, even though they cannot be systematically decoupled [7,8]. In the following, the focus is made on normal impacts. Before any consideration on adhesion forces can be made, it is important to introduce the concept of adhesion criterion. The outcome of a collision between a dust particle and a surface is characterized by the *adhesion velocity,* v_{adh}. For impact velocities above v_{adh}, rebound is possible and usually comes with significant energy loss because of plastic deformation and the work of adhesion forces. When there is rebound, restitution coefficients (defined as the ratio of a given quantity after and before the collision event) are needed to characterize the dust after impact. If the dust normal impact velocity v_0 is below v_{adh}, it will stick to the surface as adhesion forces are strong enough to prevent rebound. In this case, the quantification of the adhesion force is critical to predict dust remobilization. The first attempt to model dust-wall collisions in tokamaks was made in the DUSTT code, where constant restitution coefficients for the dust size and temperature were used [9]. In a later work, constant restitution coefficients for the normal velocity were combined with a constant probability for adhesion [2]. DUSTT was also coupled to a finite element code in order to study the special case of high velocity impacts ($v_0 \sim 0.1 - 1$ km/s) [10]. The MIGRAINe code implements the most complete analytical dust-wall collisions model to date [11]. The adhesion velocity and velocity restitution coefficients are calculated using the Thornton and Ning (T&N) model for the normal impact of elastic-perfectly plastic adhesive spheres [12]. This model was validated against experimental measurements of velocity restitution coefficients for impacts close to normal incidence [13,14]. When the dust sticks to the surface, the quantification of the adhesion force is primordial. Due to adhesion forces and irreversible plastic deformation accumulated during the impact, a once spherical particle exhibits a non-zero contact area with the surface. This contact radius, a, depends on the dust impact velocity when plastic deformation is present. This was demonstrated experimentally for tokamak-relevant materials and impact velocities [15]. Since it was shown that Tungsten (W) exhibits a perfectly plastic behavior [16], a can be calculated using the T&N model for the normal impact of elastic-perfectly plastic adhesive spheres, since the force-displacement curve can be linearized [17]. Thus one can estimate the contact radius at the end of the loading-unloading cycle as a function of the impact velocity. Once a is known, the adhesion force can be calculated from the van der Waals potential [18]. The well-known van der Waals force expression is obtained for spherical particles at close range with a planar surface, hence the need for a calculation involving a more complex dust shape. In this paper, we first recall the basics of particle adhesion on planar surfaces. Applied in the case of W/W impacts, we show that plasticity plays a predominant role in dust-wall collisions. When there is adhesion, we estimate the contact radius, focusing on its dependence on the impact velocity. Then, an

* Corresponding author.
E-mail address: adrien.autricque@cea.fr (A. Autricque).

https://doi.org/10.1016/j.nme.2019.02.001
Received 15 November 2018; Received in revised form 31 January 2019; Accepted 1 February 2019
Available online 11 February 2019

expression of the van der Waals adhesion force on such a deformed dust particle is proposed. The importance of the impact velocity on the adhesion force is emphasized. The effects of the surface roughness is also studied.

2. The omnipresence of plastic deformations for W/W impacts

When a dust particle hits a flat surface, its initial kinetic energy is converted into elastic (and, possibly, plastic) deformation energy, adhesion work and other dissipation mechanisms such as viscoelastic effects. Rebound occurs if the elastic deformation energy returned during the unloading phase is sufficient to overcome the adhesion work. Let us consider a spherical dust grain of radius r_d impacting a flat surface. Subscripts d and s are used for parameters of the dust grain and the substrate, respectively. The adhesion velocity can be calculated in the framework of the Johnson–Kendall–Roberts (JKR) theory [19], where it is defined by

$$v_{\text{adh}}^{\text{JKR}} = \sqrt{\frac{3}{5}(1 + 6 \times 2^{2/3})}\left(\frac{\pi^2\gamma^5}{2\rho_d^3 E_*^2 r_d^5}\right)^{1/6}, \tag{1}$$

where ρ_d is the dust density, $\gamma = \sqrt{\gamma_d\gamma_s}$, γ_i being the surface energies and E_* is the reduced Young modulus defined by

$$\frac{1}{E_*} = \frac{1-\nu_d^2}{E_d} + \frac{1-\nu_s^2}{E_s}, \tag{2}$$

where E_i and ν_i are the Young moduli and Poisson ratios, respectively. This criterion accounts for elastic deformation only, and gives $v_{\text{adh}}^{\text{JKR}} = 1.34$ m/s for a W/W impact and $r_d = 1$ µm. Material parameters used throughout this paper are summarized in Table 1.

If plastic deformation is to be incorporated in the picture, there exists a minimal impact velocity above which there is enough energy in the system to set off plastic deformation. This so-called yield velocity, v_y, is calculated using the T&N model, which considers the normal impact of elastic-perfectly plastic adhesive spheres [12]

$$v_y = \frac{\pi^2}{2\sqrt{10}}\sqrt{\frac{p_y^5}{\rho_d E_*^4}}, \tag{3}$$

where p_y is the yield pressure, which usually ranges between $1.6\sigma_y$ and $2.8\sigma_y$, σ_y being the material yield strength [11]. In the following, we arbitrarily choose $p_y = 2\sigma_y$. In the case of a W/W impact, one finds $v_y = 7.5$ mm/s, which is rather small when compared to typical dust velocities in tokamaks [10]. Moreover, in the case of W/W impacts, v_y is systematically lower than $v_{\text{adh}}^{\text{JKR}}$, which means that plastic deformation are always at play during impacts, and the JKR theory is inapplicable. The adhesion criterion accounting for plastic dissipation can be obtained from the T&N model for the normal impact of elastic-perfectly plastic adhesive spheres. It is determined by equating the restitution coefficient given by the T&N model to zero, as was done in Ref. [11]. One finds that the adhesion velocity is the solution of the following equation

Table 1
W material parameters used in this paper.

Name	Symbol	Value	Ref.
Surface energy	γ	4.36 J/m^2	[20]
Young modulus	E	400 GPa	[21]
Poisson ratio	ν	0.29	[21]
Yield strength	σ_y	500 MPa	[16]
Density	ρ	19.2 g/cm^3	[22]
Hamaker constant	A	4.9×10^{-19} J	[23,24]

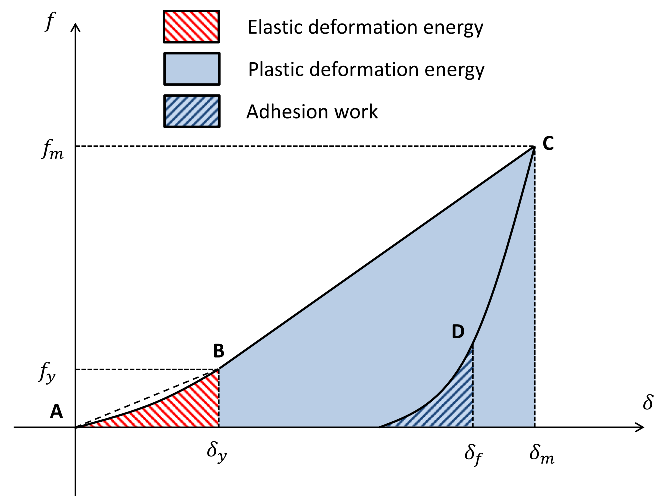

Fig. 1. Sketch of the force - overlap curve for the impact of an elastic perfectly-plastic adhesive sphere. Three phases are distinguishable: elastic (AB) and plastic (BC) loading and elastic unloading (CD).

$$\left(\frac{v_{\text{adh}}^{\text{JKR}}}{v_y}\right)^2\left(\frac{v_y}{v_{\text{adh}}}\right)^{3/2}\left[\frac{v_y}{v_{\text{adh}}} + \frac{2}{\sqrt{5}}\sqrt{6 - \left(\frac{v_y}{v_{\text{adh}}}\right)^2}\right]^{1/2} = \frac{6\sqrt{3}}{5}\left[1 - \frac{1}{6}\left(\frac{v_y}{v_{\text{adh}}}\right)^2\right]. \tag{4}$$

For a W/W impact with $r_d = 1$ µm, one finds $v_{\text{adh}} = 6.03$ m/s, which is much higher than v_y. Dissipation phenomena other than plasticity (such as viscoelastic effects) could even further increase the adhesion criterion [25]. In the following, we focus on the case of W/W impacts and in the regime where $v_y \ll v_0 \le v_{\text{adh}}$, which should represent most of the dust impact velocities encountered in tokamaks [10]. In this regime, the deformation energy is dominated by plasticity, meaning that the contact radius is a function of the impact velocity.

3. Estimation of the contact radius for sticking W grains

When a spherical dust particle impacts and sticks to a flat surface, it is elastoplastically deformed. The kinetics of an adhesive dust-surface normal impact for an elastic-perfectly plastic adhesive sphere is divided into the loading and unloading phases, as can be seen in Fig. 1. δ designates the overlap (indentation depth), with $\delta = a^2/r_d$. During the loading phase, the dust initial kinetic energy is converted into elastic deformation energy (AB) until the yield (elastoplastic transition) is reached (if $v_0 \ge v_y$). Then, the remaining energy is converted into irreversible plastic deformation (BC). If the material is perfectly plastic, the force f increases linearly with δ since the pressure saturates at p_y (and the force increase is solely dictated by the contact radius increase). When all the dust initial kinetic energy is converted into deformation energy, δ has reached its maximal value δ_m. During the unloading phase (CD), the material elastically unloads until the remaining elastic deformation energy equals the adhesion work. At the end of the cycle, there is a residual overlap δ_f due to both adhesion work and irreversible plastic deformation. Since the amount of plastic deformation depends on the impact velocity, so does the final overlap. In this section, the final contact radius is determined as a function of the impact velocity. First, if the impact velocity is exactly v_y, the dust kinetic energy equals the full elastic deformation energy, which can be approximated by

$$\frac{1}{2}m_d v_y^2 \approx \frac{1}{2}k_e\delta_y^2, \tag{5}$$

where k_e is the elastic stiffness of the material. The yield force can be linked to the yield pressure with $f_y = k_e\delta_y = p_y\pi r_d\delta_y$, and we can deduce the yield overlap

$$\delta_y = \frac{r_d}{\sqrt{30}}\left(\frac{\pi p_y}{E_*}\right)^2. \tag{6}$$

In the regime of impact velocities considered, the elastic deformation energy (in the loading phase) is negligible with respect to the plastic deformation energy, which in turn equals the dust initial kinetic energy

$$\frac{1}{2}m_d v_0^2 \approx \frac{1}{2}(\delta_m - \delta_y)(f_m + f_y) \approx \frac{1}{2}\delta_m(f_m + f_y), \tag{7}$$

since $\delta_m \gg \delta_y$. Also, since W is perfectly plastic [16], the force-overlap law in the plastic domain (BC) is linear and the evolution of the force is solely dictated by the increase of the contact radius, i.e., $f_m = p_y \pi r_d \delta_m$. We obtain

$$\left(\frac{\delta_m}{\delta_y}\right)^2 + \frac{\delta_m}{\delta_y} \approx \left(\frac{\delta_m}{\delta_y}\right)^2 = \left(\frac{v_0}{v_y}\right)^2. \tag{8}$$

This expression is valid as long as the deformation remains small, i.e., $\delta_m \ll r_d$, which is equivalent to the impact velocity being small compared to $v_{\max} = \sqrt{3p_y/(4\rho_d)} = 198$ m/s, which is much higher than adhesion velocities for tokamak dust. Thus the deformation should remain small as long as the dust sticks to the surface. The elastic unloading (CD) is also negligible due to the high elastic stiffness of W. Thus the final contact radius is close to the maximal value $a_m = \sqrt{r_d \delta_m}$. In this light

$$a = r_d\left(\frac{4\rho_d v_0^2}{3p_y}\right)^{1/4}. \tag{9}$$

For a 1 µm dust with $v_0 = 1$ m/s, $a = 71$ nm. As a reminder, the JKR contact radius is

$$a_{\mathrm{JKR}} = \left(\frac{9\pi\gamma r_d^2}{E_*}\right)^{1/3}, \tag{10}$$

which is 82 nm with the same parameters as above. Thus, even though the two models are not comparable, they give results of the same order of magnitude.

4. Van der Waals adhesion force on a deformed dust grain

In this Section, we attempt to describe the van der Waals force acting on a dust grain deformed by its impact with the surface. We consider the dust to be located at a distance H from the surface and assume the dust to be deformed only at the contact area while keeping its spherical shape elsewhere. This assumption is valid if the deformation remains small (δ, $a \ll r_d$), which was demonstrated in Section 3. A schematic view of the configuration is shown in Fig. 2.

4.1. Calculation of the van der Waals force

The van der Waals interaction potential between a planar surface

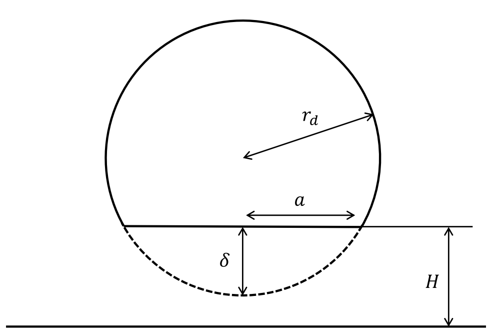

Fig. 2. Schematic of the deformation of the dust grain. Dimensions are deliberately exaggerated.

and the truncated sphere represented in Fig. 2 is written [18]

$$U(r) = -\frac{A}{6}\int_{\delta}^{2r_d} \frac{r_d^2 - (x - r_d)^2}{(r + x)^3}dx, \tag{11}$$

where $r = H - \delta$ and A is the Hamaker constant. After integration, the van der Waals adhesion force is obtained by $F_{\mathrm{VdW}} = -dU/dr$, i.e.,

$$F_{\mathrm{VdW}} = -\frac{Ar_d}{6H^2}\left[\frac{H+\delta}{H-\delta} + \left(\frac{H}{H-\delta+2r_d}\right)^2 + H\frac{\delta - 2r_d}{r_d(H-\delta+2r_d)} - \frac{\delta}{r_d} - \delta^2\frac{H-\delta+2r_d}{r_d H(H-\delta)}\right]. \tag{12}$$

In the case of a spherical (non-deformed) particle ($\delta = a = 0$), we obtain

$$F_{\mathrm{VdW}}(\delta = 0) = -\frac{2Ar_d^3}{3H^2(H+2r_d)^2}. \tag{13}$$

When at close range of the surface ($H \ll r_d$), we recover the well-known expression for the van der Waals force

$$F_{\mathrm{VdW}}(\delta = 0,\, H \ll r_d) = F_0 = -\frac{Ar_d}{6H^2}. \tag{14}$$

In the general case ($\delta \neq 0$), we make two simplifying assumptions. The first one is that the dust is in contact with the surface, i.e., $H = H_0 \approx 0.36$ nm $\ll r_d$ is the distance of closest approach [23]. This first assumption is compulsory, since we consider the dust to have had a sticking impact with the surface. This allows us to simplify Eq. (12) to

$$F_{\mathrm{VdW}} = F_0\left(1 + \frac{2a^2}{r_d H_0}\right). \tag{15}$$

Second, for the deformed dust grain to remain spherical everywhere but at the contact area and in order to assimilate the deformed dust radius to be equal to the dust radius prior to the collision, we must assume that the deformation is small, i.e., $a \ll r_d \Rightarrow \delta \ll r_d$, which is consistent with results from Section 3. Eq. (15) implies that the adhesion force is increased from the non-deformed case. Note that we recover the expression proposed in Ref. [26]. F_{VdW}/F_0 is plotted against a/r_d for a W dust grain of radius $r_d = 1$ µm on a W substrate in Fig. 3. It appears that the adhesion force can be enhanced by up to two orders of magnitude when the dust is significantly deformed.

4.2. Accounting for the surface nanoscale roughness

Here we attempt to incorporate the effects of the roughness on Eq. (15), which should tend to reduce the adhesion force by reducing the contact area. The roughness is represented, in a similar way to the Rumpf model modified by Rabinovich et al. [27] by a hemisphere of radius r and an underlying plane. The maximum height of the asperity (with respect to the underlying plane) is called y_m, and λ is the peak-to-peak distance. As both the dust grain and the asperity are plastically deformed and share the same contact radius a, the total van der Waals force is the sum of two components: (i) the force between the deformed dust and the deformed asperity and (ii) the force between the deformed dust and the underlying plane. A schematic view of the problem is represented in Fig. 4.

The exact same calculation as detailed in Section 4.1 can be done in the case of two deformed spheres of radii R_1 and R_2 sharing the same contact area of radius a. The van der Waals force between these two spheres is, when H_0, $a \ll R_1, R_2$,

$$F_{\mathrm{VdW}} = \frac{A}{6H_0^2}\left(\frac{R_1R_2}{R_1+R_2} + \frac{2a^2}{H_0}\right). \tag{16}$$

This calculation is easily performed using the same method as in Ref. [18]. Also, the contact radius between these two spheres can be calculated the same way as in Section 3. One finds

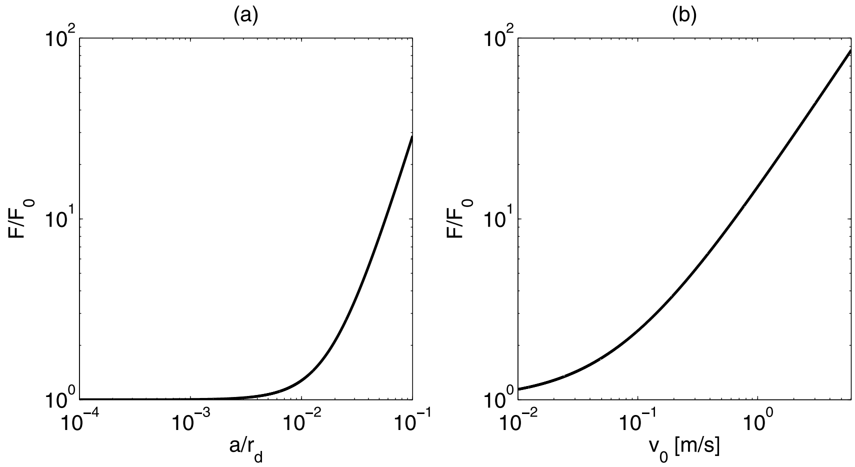

Fig. 3. Van der Waals force on a deformed W dust grain against the contact radius (a) and the impact velocity (b) for $r_d = 1$ µm.

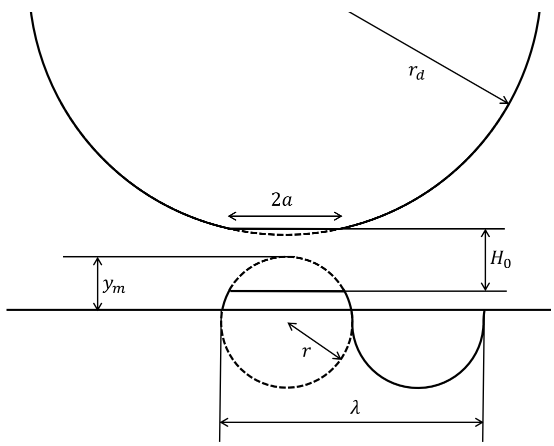

Fig. 4. Schematic of the deformation of the dust grain and the asperity when the surface is rough. Dimensions are deliberately exaggerated.

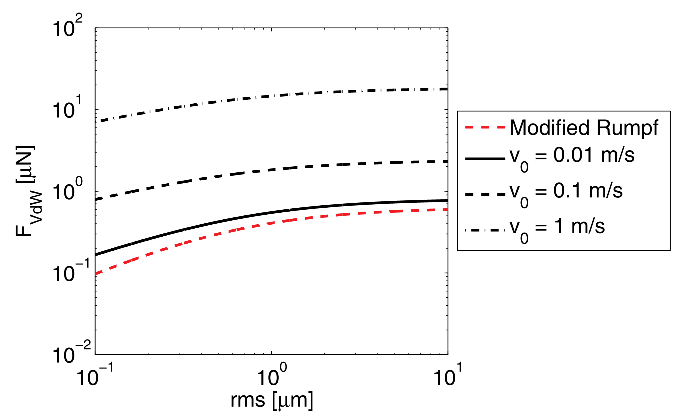

Fig. 5. Van der Waals force from Eq. (20) on a W dust grain laying on a rough W surface against the rms for $r_d = 1$ µm and for varying impact velocities. The value given by the modified Rumpf model, Eq. (20) with $a = 0$, is shown as a comparison.

$$a = \left(\frac{2E_0}{\pi p_y}\frac{R_1 R_2}{R_1 + R_2}\right)^{1/4}, \tag{17}$$

where E_0 is the initial kinetic energy of one of the two bodies, the other being considered immobile. Eq. (17) can be rewritten, with $R_1 = r_d$, $R_2 = r$ and $E_0 = m_d v_0^2/2$,

$$a = r_d\left[\frac{4\rho_d v_0^2}{3p_y(1 + r_d/r)}\right]^{1/4}. \tag{18}$$

Using the same calculation as in Ref. [27], the total van der Waals force is

$$F_{\mathrm{VdW}} = -\frac{Ar_d}{6H_0^2}\left[\frac{r}{r_d + r} + \frac{2a^2}{r_d H_0}\right] - \frac{Ar_d}{6(H_0 + y_m)^2}\left[1 + \frac{2a^2}{r_d(H_0 + y_m)}\right], \tag{19}$$

where the two terms correspond to the contributions (i) and (ii) detailed at the beginning of this Section, respectively. It is more convenient to express the force in terms of root mean square (rms) roughness and peak-to-peak distance λ. From Ref. [27], we have $r \approx \lambda^2/(58\mathrm{rms})$ and $y_m \approx 1.82\mathrm{rms}$. Rearranging, we find

$$F_{\mathrm{VdW}} = F_0\left[\frac{1}{1 + 58r_d\mathrm{rms}/\lambda^2} + \frac{1}{(1 + 1.82\mathrm{rms}/H_0)^2} + \frac{2a^2}{r_d H_0}\left(1 + \frac{1}{(1 + 1.82\mathrm{rms}/H_0)^3}\right)\right]. \tag{20}$$

Note that we recover the expression from Rabinovich et al. for a non-deformed dust ($a = 0$) and the modified Rumpf model in the particular case where the center of the asperity coincides with the underlying plane ($y_m = r$). F_{VdW} from Eq. (20) is plotted in Fig. 5 against rms in the case $y_m = r$ and for various values of dust impact velocities. When $v_0 = 0$, $a = 0$ and Eq. (20) reduces to the modified Rumpf model. Eq. (20)is valid for relatively rough surfaces, i.e., when $r \gtrsim r_d$, because the deformation of the dust due to contact with the underlying plane is not considered. In this regime, the sphere-sphere interaction dominates over the sphere-plane. In tokamaks, one can expect such high values of roughness due to surface erosion by the plasma [28]. It appears that the adhesion force can be significantly increased when compared to the modified Rumpf model, even at low impact velocities, as $v_0 \sim 1$ m/s corresponds to a free fall in vacuum from a ~ 10 cm height. This highlights the high sensitivity of the adhesion force to the way the dust was deposited onto the substrate. Moreover, the values of forces obtained are in quantitative agreement with adhesion force measurements performed on W dust, as the reduction of adhesion force due to the surface roughness can be compensated by an increase due to deformation of the bodies upon impact [29,30].

5. Conclusion

New insights on W dust adhesion on W tokamak plasma-facing surfaces have been presented. When adhered to a surface with an impact velocity, a W dust grain is elastically and perfectly plastically deformed. A new expression for the van der Waals force acting on a deformed dust particle laying on a perfectly smooth surface has been derived. The link between adhesion force and impact velocity has been made. We showed that the adhesion force can be enhanced by up to two orders of magnitude with respect to the classical van der Waals expression in the ideal case of perfectly smooth surface for reasonable dust impact velocities that may be encountered in tokamaks. On the other hand, reduction of the adhesion force due to surface roughness has been estimated using a method similar to the Rumpf model and an expression applicable to parameter regimes relevant to fusion devices has been presented. This final expression was shown to be in reasonable agreement with adhesion force measurements, since the increase of adhesion force due to effects of the impact velocity can be compensated by a reduction due to the surface roughness. Our results stress that, when performing adhesion force measurements with W, the velocity at which the dust is deposited on the surface as well as the surface roughness are critical parameters to the outcome of the experiment.

References

[1] S.I. Krasheninnikov, R.D. Smirnov, D.L. Rudakov, Dust in magnetic fusion devices, Plasma Phys. Controlled Fusion 53 (8) (2011) 083001.

[2] R.D. Smirnov, A.Y. Pigarov, M. Rosenberg, S.I. Krasheninnikov, D.A. Mendis, Modelling of dynamics and transport of carbon dust particles in tokamaks, Plasma Phys. Controlled Fusion 49 (4) (2007) 347.

[3] M. Bacharis, M. Coppins, J.E. Allen, Dust in tokamaks: an overview of the physical model of the dust in tokamaks code, Phys. Plasmas 17 (2010) 042505, https://doi.org/10.1063/1.3383050.

[4] E. Lazzaro, I. Proverbio, F. Nespoli, S. Ratynskaia, C. Castaldo, U. deAngelis, M. DeAngeli, J.-P. Banon, L. Vignitchouk, Transport and effects of ferromagnetic dust in a tokamak with a metallic vessel, Plasma Phys. Controlled Fusion 54 (12) (2012) 124043.

[5] L. Vignitchouk, P. Tolias, S. Ratynskaia, Plasma Phys. Controlled Fusion 56 (9) (2014) 095005.

[6] A. Autricque, S. Hong, N. Fedorczak, S. Son, H. Lee, I. Song, W. Choe, C. Grisolia, Nucl. Mater. Energy 12 (Suppl. C) (2017) 599. Proceedings of the 22nd International Conference on Plasma Surface Interactions 2016, 22nd PSI

[7] R.M. Brach, P.F. Dunn, X. Li, J. Adhes. 74 (1–4) (2000) 227, https://doi.org/10.1080/00218460008034531.

[8] A.G. Konstandopoulos, J. Aerosol. Sci. 37 (3) (2006) 292.

[9] A.Y. Pigarov, S.I. Krasheninnikov, T.K. Soboleva, T.D. Rognlien, Phys. Plasmas 12 (2005) 122508.

[10] R. Smirnov, S. Krasheninnikov, A. Pigarov, D. Benson, M. Rosenberg, D. Mendis, J. Nucl. Mater. 390–391 (2009) 84. Proceedings of the 18th International Conference on Plasma-Surface Interactions in Controlled Fusion Device.

[11] S. Ratynskaia, L. Vignitchouk, P. Tolias, I. Bykov, H. Bergsker, A. Litnovsky, N. den Harder, E. Lazzaro, Nucl. Fusion 53 (12) (2013) 123002.

[12] C. Thornton, Z. Ning, Powder Technol 99 (2) (1998) 154.

[13] S. Ratynskaia, P. Tolias, A. Shalpegin, L. Vignitchouk, M.D. Angeli, I. Bykov, K. Bystrov, S. Bardin, F. Brochard, D. Ripamonti, N. den Harder, G.D. Temmerman, J. Nucl. Mater. 463 (2015) 877. Plasma-surface interactions 21.

[14] P. Tolias, S. Ratynskaia, A. Shalpegin, L. Vignitchouk, F. Brochard, M.D. Angeli, H. van der Meiden, Nucl. Mater. Energy 12 (2017) 524. Proceedings of the 22nd International Conference on Plasma Surface Interactions 2016, 22nd PSI.

[15] P. Tolias, G. Riva, M.D. Angeli, S. Ratynskaia, G. Daminelli, C. Lungu, C. Porosnicu, Nucl. Mater. Energy 15 (2018) 55.

[16] M. Wirtz, I. Uytdenhouwen, V. Barabash, F. Escourbiac, T. Hirai, J. Linke, T. Loewenhoff, S. Panayotis, G. Pintsuk, Nucl. Fusion 57 (6) (2017) 066018.

[17] M. Pasha, S. Dogbe, C. Hare, A. Hassanpour, M. Ghadiri, Granular Matter 16 (1) (2014) 151.

[18] H. Hamaker, Physica 4 (10) (1937) 1058.

[19] K.L. Johnson, K. Kendall, A.D. Roberts, Proc. R. Soc. Lond. 324 (1558) (1971) 301.

[20] W. Huisl, G. Czack, G. Kirschstein, W. Kurtz, F. Stein, W tungsten: supplement volume A4 surface properties. electron emission, Gmelin Handbook of Inorganic and Organometallic Chemistry, eighth ed., Springer Berlin Heidelberg, 2013.

[21] R. Lowrie, A.M. Gonas, J. Appl. Phys. 36 (7) (1965) 2189, https://doi.org/10.1063/1.1714447.

[22] W. Haynes, CRC Handbook of Chemistry and Physics, 94th ed., 100 Key Points, CRC Press, 2016.

[23] J.N. Israelachvili, J.N. Israelachvili, Intermolecular and Surface Forces (Third Edition), third ed., Academic Press, Boston, 2011, p. 253.

[24] P. Tolias, Fusion Eng. Des. 133 (2018) 110.

[25] S. Chen, S. Li, M. Yang, Powder Technol 274 (Suppl. C) (2015) 431.

[26] S. Alvo, P. Lambert, M. Gauthier, S. Rgnier, J. Adhes. Sci. Technol. 24 (15,16) (2010) 2415, https://doi.org/10.1163/016942410X508334.

[27] Y.I. Rabinovich, J.J. Adler, A. Ata, R.K. Singh, B.M. Moudgil, J. Colloid Interface Sci. 232 (1) (2000) 10.

[28] C. Stancu, F. Stokker-Cheregi, A. Moldovan, M. Dinescu, C. Grisolia, G. Dinescu, Appl. Phys. A 123 (10) (2017) 618.

[29] S. Peillon, M. Sow, C. Grisolia, F. Miserque, F. Gensdarmes, J. Electrostat. 88 (Suppl. C) (2017) 111. Special Issue on The International Conference on Electrostatics, Electrostatics 2017.

[30] G. Riva, P. Tolias, S. Ratynskaia, G. Daminelli, R. Donde, M.D. Angeli, E. Vassallo, M. Pedroni, Nuclear materials and energy, Proceedings of the 22nd International Conference on Plasma Surface Interactions 2016, 22nd PSI, 12 (2017), p. 593.